Proc. Natl. Acad. Sci. USA
Vol. 87, pp. 3675–3679, May 1990
Biochemistry

Binding of substrate CO_2 to the active site of human carbonic anhydrase II: A molecular dynamics study

(zinc enzyme/binding pathway/enzyme–substrate interaction)

JIIN-YUN LIANG AND WILLIAM N. LIPSCOMB

Gibbs Chemical Laboratories, Department of Chemistry, Harvard University, Cambridge, MA 02138

Contributed by William N. Lipscomb, February 15, 1990

ABSTRACT **Molecular dynamics has been used to study binding of substrate CO_2 to the active site of human carbonic anhydrase II. Three potential CO_2 binding sites have been located. The first is at the active-site hydrophobic pocket (the catalytically productive site), where CO_2 is ≈3.5 Å from the zinc ion and interacts with His-94, His-119, Val-121, Val-143, Leu-198, Thr-199, the zinc ion, and the zinc-bound hydroxide ion. The second CO_2 binding site is ≈6 Å from the zinc ion, where CO_2 interacts with His-64, His-94, Leu-198, Thr-200, Pro-201, Pro-202, and some active-site water molecules. The third CO_2 binding site is ≈10 Å from the zinc ion, is largely solvated by water molecules, and interacts with His-64, Asn-67, and Gln-92. At these three CO_2 binding sites, the CO_2 molecule is highly localized (the average Zn—CO_2 distance fluctuation is ≈1 Å) and favors the linear binding orientation toward the zinc ion. This linear binding orientation of CO_2 and its electrostatic interaction with the zinc ion direct diffusion of CO_2 toward the zinc ion and facilitate the nucleophilic attack from O of the zinc-bound OH^- to C of CO_2 in the productive hydrophobic binding site. Finally, the two CO_2 binding sites outside the hydrophobic binding pocket, which may represent two intermediate states along the CO_2 binding pathway, could play important roles as a CO_2 relay.**

Human carbonic anhydrase II (HCA II) is a zinc-metalloenzyme that catalyzes the reversible hydration of CO_2 and is responsible for fast metabolism of CO_2 in the human body. The enzyme's active site is a conical cavity, which is about 15 Å wide at the entrance and 16 Å deep. The zinc ion, located near the apex of the cone, has three histidine ligands from the protein, and a solvent water molecule is bound at the fourth coordination site. The active site can be divided into the hydrophobic region, which includes Trp-209, Val-143, and other hydrophobic residues, and the hydrophilic region, which includes Glu-106, Thr-199, the partially ordered active-site water molecules, and His-64. It is thought that the hydrophobic region is important for substrate binding and that the hydrophilic region participates in the deprotonation step in the enzyme-catalyzed CO_2 hydration (for review articles, see refs. 1–8).

Here, we are interested in applying molecular dynamics methods to examine the first step of carbonic anhydrase-catalyzed CO_2 hydration, which involves CO_2 binding in the active site of HCA II. Experimentally, the low solubility of CO_2 in aqueous solution and the fast turnover number of carbonic anhydrase-catalyzed CO_2 hydration have prevented any direct observation of feasible CO_2 binding sites.

Experimental results, such as ^{13}C NMR studies of ^{13}C-labeled HCO_3^- binding to Co^{2+}-substituted HCA I (9, 10) and x-ray crystallographic studies of enzyme–inhibitor complexes with imidazole (11), sulfonamidates (12), and thiocyanate (12), suggest that CO_2 displaces the so called "deep" water and binds within the hydrophobic pocket near the metal ion. However, a description at the molecular level of the binding mechanism and binding interactions of substrate CO_2 at the enzyme's active site is still lacking. Below, we report the results of a detailed study of CO_2 binding to the active site of HCA II.

METHODS

The molecular dynamics/x-ray crystallographic refinement program XPLOR (13) was used to perform the molecular dynamics simulations. The initial position of substrate CO_2 was obtained by replacing the position of inhibitor SCN^- at the active site hydrophobic pocket in the x-ray crystallographic structure of the HCA II–SCN^- complex (12). All hydrogen atoms of the enzyme are included in our dynamical simulations. The TIP3P water model (15) was used to represent the 172 crystallographically located solvent water molecules. van der Waals' parameters, σ and ε, for the 2+-charged zinc ion were varied between 1.95 and 3.4 Å (σ) and −0.04 and −0.25 kcal/mol (ε) (1 cal = 4.184 J), respectively, to investigate their effects on the dynamical results. This zinc ion is bonded to its three histidine ligands and a fourth OH^- ligand in a tetrahedral geometry. Other parameters include the bond force constants of 500 kcal/mol·Å^2 for Zn—N(His) and 300 kcal/mol·Å^2 for Zn—O(OH^-), and the angle force constants of 70.0 kcal/mol·deg^2 for N(His)—Zn—N(His) and 50.0 kcal/mol·deg^2 for O(OH^-)—Zn—N(His). The bond force constant of C—O of the CO_2 molecule is 450 kcal/mol·Å^2, and the molecule has a fixed linear arrangement. The geometry and atomic charges of CO_2 are obtained from 6-31 + G* self-consistent field molecular orbital calculations (16). The van der Waals' parameters of C and O of CO_2 are similar to those of a carbonyl group.

In our dynamics studies, 40-psec dynamics simulations were performed to allow equilibration of CO_2 binding at the hydrophobic binding site. After that, CO_2 was moved in 0.4-Å steps away from the zinc ion toward the mouth of the active site to yield a possible diffusion pathway of CO_2.† At each Zn—C(CO_2) configuration along the diffusion pathway, the Zn—C(CO_2) distance, R_{Zn-C}, was restrained to a designated value, R_0, by a biharmonic potential, P,

$$P = s[R_{Zn-C} - (R_0 + \Delta r)]^2 \qquad R_{Zn-C} > R_0 + \Delta r$$
$$= s[R_{Zn-C} - (R_0 - \Delta r)]^2 \qquad R_{Zn-C} < R_0 - \Delta r,$$

where Δr is 0.1 Å and s is the scaling factor, and a dynamics simulation was performed, which consisted of a 5-psec equilibration followed by a 5-psec dynamics trajectory. Along the CO_2 diffusion pathway, three potential CO_2 binding sites were found by removing the biharmonic restraint on

The publication costs of this article were defrayed in part by page charge payment. This article must therefore be hereby marked "*advertisement*" in accordance with 18 U.S.C. §1734 solely to indicate this fact.

Abbreviation: HCA II, human carbonic anhydrase II.

†The PATH program (14) has failed to obtain a convergent diffusion pathway of CO_2 in our earlier calculations based on a much simplified system (data not shown).

Zn—C(CO_2) at each point along the CO_2 binding pathway and allowing the system to reequilibrate. During the identification of these three CO_2 binding sites, a 14-Å-radius water sphere was added to the mouth of the cavity to include possible solvent effects, and additional 40-psec dynamics simulations were performed for each CO_2 binding site without any Zn—C(CO_2) distance restraint. In the dynamics simulations, 0.001-psec timestep and 8.0-Å nonbonded cutoff distance were used, and the simulations were performed at 300 K. Each 10-psec dynamics simulation required ≈52 hr of central processing unit time on the DEC station 3100.

RESULTS

Fig. 1*A* depicts one possible diffusion pathway of CO_2 in the active site of HCA II: the pathway begins at the entrance of the active site cavity of HCA II ≈14.0 Å from the zinc ion and ends at the hydrophobic or catalytically productive binding pocket. Table 1 gives the active site residues that are in close contact with CO_2 along the diffusion pathway, and the interaction energies between substrate CO_2 and the enzyme.‡ Along the CO_2 diffusion pathway, van der Waals' interactions between CO_2 and HCA II are more favorable than the corresponding electrostatic interactions (Table 1).

Three potential CO_2 binding sites were found along the CO_2 diffusion pathway in the dynamics simulations. They are the hydrophobic pocket, a middle binding site at a zinc–carbon distance of ≈6 Å, and an exterior binding site at ≈10 Å from the zinc ion. When CO_2 was initially positioned at Zn—C(CO_2) = 4.0–6.0 Å, removal of distance restraints and subsequent equilibration led to CO_2 binding to the middle binding site at 6 Å from the zinc ion, where CO_2 interacts with His-64, His-94, Leu-198, Thr-200, Pro-201, Pro-202, and some active-site water molecules (Fig. 1*C*). For CO_2 initially positioned at Zn—C(CO_2) greater than 6 Å and exterior to His-64, Zn—C(CO_2) relaxation and dynamical equilibration result in binding of CO_2 at the exterior binding site ≈10 Å from zinc,

‡A cutoff distance of 20.0 Å was used, and most interaction energies converged at a cutoff distance of ≈15 Å.

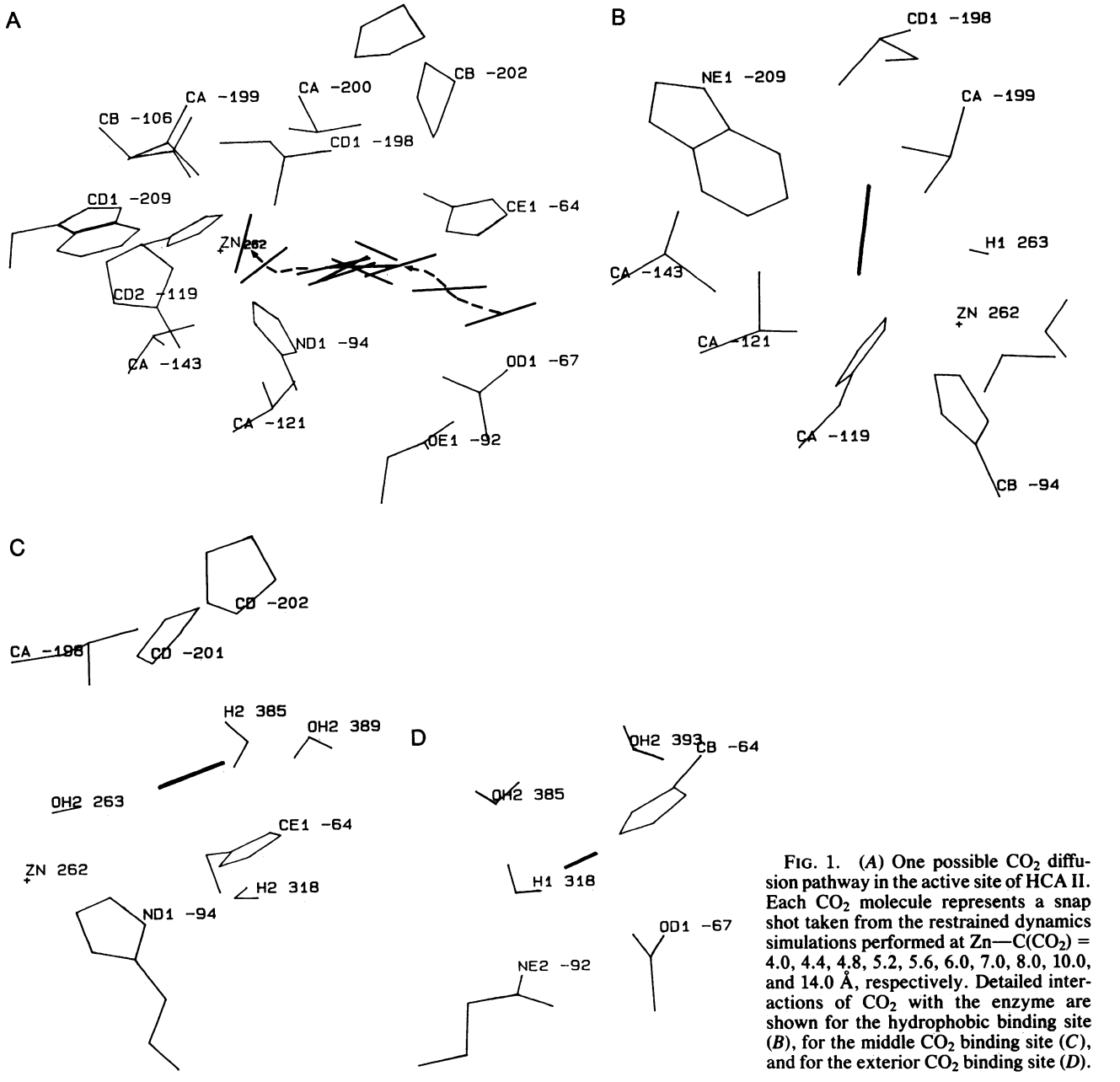

FIG. 1. (*A*) One possible CO_2 diffusion pathway in the active site of HCA II. Each CO_2 molecule represents a snap shot taken from the restrained dynamics simulations performed at Zn—C(CO_2) = 4.0, 4.4, 4.8, 5.2, 5.6, 6.0, 7.0, 8.0, 10.0, and 14.0 Å, respectively. Detailed interactions of CO_2 with the enzyme are shown for the hydrophobic binding site (*B*), for the middle CO_2 binding site (*C*), and for the exterior CO_2 binding site (*D*).

Table 1. Interaction of CO_2 with HCA II

Zn—C distance, Å	Interaction(s), kcal/mol Total	vdW	Elec	Active-site residues
3.4	−17.3	−8.2	−9.1	H-119, V-121, V-143, L-198, T-199
4.0	−12.9	−6.1	−6.8	H-94, V-121, L-198, T-199, T-200
4.4	−13.7	−7.1	−6.7	H-94, V-121, L-198, T-200
4.8	−13.7	−7.7	−6.0	H-94, V-121, L-198, T-200, P-201
5.2	−11.7	−7.2	−4.5	H-94, V-121, L-198, T-200, P-201
5.6	−9.0	−7.9	−1.1	H-94, V-121, L-198, T-200, P-201, P-202
6.0	−10.2	−8.2	−2.0	H-64, L-198, T-200, P-201, P-202
7.0	−9.1	−7.1	−1.9	H-64, L-198, T-200, P-201, P-202
8.0	−8.2	−5.6	−2.6	H-64, L-198, P-201, P-202
10.0	−17.0	−10.4	−6.6	H-64, N-67, Q-92
14.0	−4.8	−3.8	−1.0	N-67, Q-92

Active site residues are within a 4-Å distance of CO_2. The interaction energies shown here do not consider entropic effects. K. M. Merz (personal communication) has used thermodynamic perturbation methods to obtain binding free energies for CO_2 bound in the active site of HCA II. The single-letter amino acid code is used. Elec, electrostatic; vdW, van der Waals'.

where CO_2 interacts with His-64, Asn-67, Gln-92, and solvent water molecules (Fig. 1*D*). Finally, for CO_2 initially positioned near the hydrophobic pocket, the hydrophobic pocket is the ultimate CO_2 binding site, in which CO_2 interacts with His-94, His-119, Val-121, Val-143, Leu-198, Thr-199, the zinc ion, and the zinc-bound hydroxide ion (Fig. 1*B*).

Table 2 summarizes our analysis of the detailed interactions between CO_2 and various active-site residues at these three potential CO_2 binding sites. At the hydrophobic binding site, interactions of CO_2 with zinc-bound OH^-, Thr-199, and the zinc ion are primarily electrostatic, whereas interactions of CO_2 with active-site hydrophobic residues (Val-121, Val-143, Leu-198, and Trp-209) are mostly van der Waals' interactions.

At the middle CO_2 binding site, except for interactions with Pro-201 and the water molecules, van der Waals' interactions of CO_2 with the active site residues are more important than the corresponding electrostatic interactions. Finally, at the exterior CO_2 binding site, where more water molecules are present, interactions between CO_2 and solvent water molecules are more significant, and the major interactions of CO_2 with the enzyme occur at His-64, Asn-67, and Gln-92.

Fig. 2 depicts the radial and angular distribution functions of CO_2 relative to the zinc ion at the hydrophobic binding site. In Fig. 2*A*, three distinct peaks, which represent the positions of carbon and two oxygen atoms of CO_2 are found (the distance fluctuations of individual atoms are ≈1 Å). In Fig. 2*B*, CO_2 shows a statistically significant preference for the linear binding orientation with $\tau = 0°$ or $\tau = 180°$. This observed distribution of the angle τ that CO_2 makes with the vector connecting C with Zn must be contrasted with that obtained for a linear molecule randomly oriented with respect to the zinc ion. This "random" distribution has a sin τ-dependence (Fig. 2*B*), which can be derived from geometric considerations. These results suggest that binding of CO_2 near the zinc ion permits limited structural fluctuations in the binding distance and orientation of CO_2, and the linear binding orientation is strongly favored. The radial distribution functions obtained for CO_2 bound to the middle and exterior binding sites resemble those obtained at the hydrophobic binding site, except that the carbon peaks are now centered at 6.2 and 10.3 Å, respectively, and the peak widths are slightly increased (results not shown). In addition, the corresponding angular distribution functions show the same statistically significant preference for the linear binding orientation of CO_2.

Finally, we analyzed the effects of various zinc parameters on results obtained from dynamics simulations of CO_2 binding to the hydrophobic pocket by varying the van der Waals' parameters, ε and σ, of the zinc ion and the bond and angle force constants between the zinc ion and its three histidine and one solvent water ligands. For each parameter set used, the dynamics simulation consisted of a 10-psec equilibration followed by a 10-psec trajectory. Table 3 gives the σ and ε values, the bond and angle force constants, the distances between CO_2 and the nearest atoms of His-119, Val-121, Val-143, Trp-209, the zinc ion, the zinc-bound OH^-, the interaction energies between CO_2 and the enzyme and their metal, and van der Waals' and electrostatic contributions. These data show that, for most parameter sets (Table 3, parameter sets a, b, c, d, e, h, k, n, o, p, q, and r), similar CO_2 binding conformations were obtained. It is remarkable that, when bond and angle force constants between the zinc ion and its ligands are reduced (parameter sets a–e) in the

Table 2. Interaction of CO_2 with the enzyme at the three potential CO_2 binding sites

Hydrophobic binding site					Middle CO_2 binding site					Exterior CO_2 binding site				
Residue or moiety	Distance, Å	Interaction(s) Total	vdW	Elec	Residue or moiety	Distance, Å	Interaction(s) Total	vdW	Elec	Residue or moiety	Distance, Å	Interaction(s) Total	vdW	Elec
His-94	2.45	0.2	0.0	0.2	His-64	3.97	−1.2	−0.9	−0.4	His-64	2.91	−0.1	−0.9	−0.8
His-119	2.78	−0.7	−0.9	0.2	His-94	2.76	−0.3	−0.6	0.3	Asn-67	3.33	−3.2	−1.3	−1.9
Val-121	2.95	−0.6	−0.8	0.1	Val-121	3.61	−0.4	−0.5	0.1	Gln-92	2.85	−0.3	−1.0	0.7
Val-143	2.95	−0.7	−0.7	0.0	Leu-198	3.66	−0.8	−0.8	−0.0	H_2O	2.23	−2.1	0.1	−2.2
Leu-198	2.50	−1.0	−0.7	−0.3	Thr-200	2.90	−1.5	−0.8	0.7	H_2O	3.41	−1.1	−0.4	−0.7
Thr-199	2.42	−2.6	−1.7	−0.8	Pro-201	3.74	−1.8	−0.7	−1.1	H_2O	3.15	−1.0	−0.4	−0.6
Thr-200	3.17	0.0	−0.8	0.8	Pro-202	3.72	−0.5	−0.3	−0.2	H_2O	3.24	−0.6	−0.3	−0.3
Trp-209	3.07	−1.1	−1.0	−0.1	OH-263	2.75	2.8	−0.3	3.2	H_2O	3.41	−0.5	−0.5	−0.0
Zn-262	3.49	−1.4	−0.2	−1.2	H_2O	3.82	−0.7	−0.4	−0.3	H_2O	3.53	−1.2	−0.5	−0.8
OH-263	3.12	−6.3	0.6	−6.8	H_2O	2.46	−0.5	−0.0	−0.5	H_2O	3.59	−2.1	−0.5	−1.6
Total		−17.3	−8.2	−9.1	Total		−10.2	−8.2	−2.0	Total		−17.0	−10.4	−6.6

Distances are between CO_2 and the nearest atoms of the specified active site components. The total interaction energies (expressed as kcal/mol) between CO_2 and the enzyme may not equal to the sum of individual interaction energies listed above them, because only important CO_2–active-site residue interactions are included. Elec, electrostatic; vdW, van der Waals'.

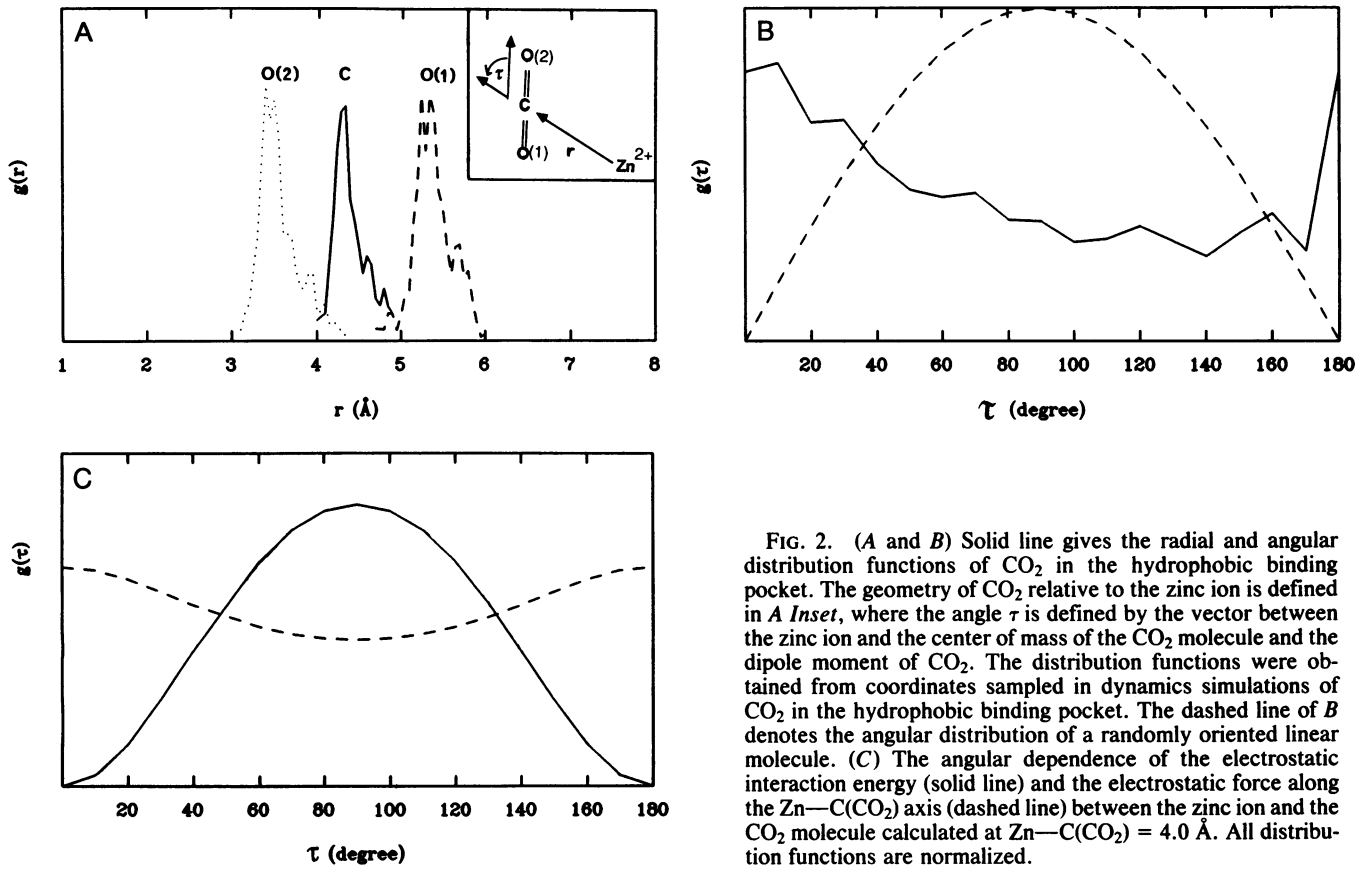

FIG. 2. (*A* and *B*) Solid line gives the radial and angular distribution functions of CO_2 in the hydrophobic binding pocket. The geometry of CO_2 relative to the zinc ion is defined in *A Inset*, where the angle τ is defined by the vector between the zinc ion and the center of mass of the CO_2 molecule and the dipole moment of CO_2. The distribution functions were obtained from coordinates sampled in dynamics simulations of CO_2 in the hydrophobic binding pocket. The dashed line of *B* denotes the angular distribution of a randomly oriented linear molecule. (*C*) The angular dependence of the electrostatic interaction energy (solid line) and the electrostatic force along the Zn—C(CO_2) axis (dashed line) between the zinc ion and the CO_2 molecule calculated at Zn—C(CO_2) = 4.0 Å. All distribution functions are normalized.

presence of fixed van der Waals' parameters, $\varepsilon = -0.25$ kcal/mol and $\sigma = 1.95$ Å, for the zinc ion, similar CO_2 binding conformations were obtained. The observed minor differences in interaction energies may be due to different positional adjustment of residues in the hydrophobic pocket in response to different bond and angle parameters. For $\sigma >$ 1.95 Å, which includes $\varepsilon = -0.25$ kcal/mol, $\sigma = 3.0$ (parameter set i) or 3.37 Å (parameter set l) and $\varepsilon = -0.043$ kcal/mol and $\sigma = 3.37$ Å (parameter set s), reduction of bond and angle force constants from 500 kcal/mol·Å^2 and 70 kcal/mol·deg^2 to 50 kcal/mol·Å^2 and 10 kcal/mol·deg^2, respectively, leads to CO_2 leaving the hydrophobic pocket to bind to the middle

Table 3. Effects of various zinc parameters on CO_2 binding in the active-site hydrophobic pocket

Parameter set	ε, kcal/mol	σ, Å	Bond	Angle	Solv	Distance from CO_2, Å						Interaction(s)			
						Zn	His-119	Val-121	Val-143	Trp-209	OH-263	Total	vdW	Elec	Zinc
a	−0.25	1.95	500.0	70.0	+	3.85	2.77	3.17	3.02	3.13	3.93	−17.2	−10.5	−6.7	−3.5
b	−0.25	1.95	250.0	10.0	+	4.61	3.61	2.97	2.75	2.90	4.16	−11.1	−10.2	−0.9	−2.8
c	−0.25	1.95	50.0	50.0	+	4.70	3.72	2.60	2.85	3.01	4.73	−11.5	−10.0	−1.5	−2.2
d	−0.25	1.95	50.0	10.0	+	4.90	3.94	2.71	3.17	3.09	3.61	−12.0	−9.0	−2.8	−2.1
e	−0.25	1.95	0.0	0.0	+	4.93	4.08	2.84	2.84	3.00	3.69	−14.2	−11.1	−3.2	−3.7
f*	−0.25	2.5	0.0	0.0	+	7.53	5.31	2.80	2.96	3.19	2.54	−10.6	−8.8	−1.8	−0.8
g*	−0.25	2.2	0.0	0.0	+	7.68	4.53	2.81	3.03	3.01	3.01	−13.2	−10.4	−2.8	−0.6
h	−0.25	3.0	500.0	70.0	+	3.51	2.86	3.24	3.16	3.15	3.28	−18.8	−10.3	−8.6	−4.0
i†	−0.25	3.0	50.0	10.0	+	6.47	5.67	3.14	4.43	5.05	4.31	5.1	4.6	0.4	0.5
j*	−0.25	3.0	0.0	0.0	+	8.77	4.17	2.94	2.76	2.82	3.14	−11.5	−10.0	−1.5	−0.0
k	−0.25	3.37	500.0	70.0	+	3.59	2.96	3.15	2.98	3.08	3.51	−20.1	−11.1	−9.0	−3.7
l†	−0.25	3.37	50.0	10.0	+	5.43	5.88	3.96	5.20	5.09	4.14	−11.6	−6.6	−5.1	−1.7
m*	−0.25	3.37	0.0	0.0	+	4.95	3.77	2.58	2.99	2.97	4.31	−14.9	−11.3	−3.6	−3.2
n	−0.043	3.37	500.0	70.0	+	3.49	2.78	2.93	2.95	3.07	3.15	−16.9	−8.7	−8.2	−1.7
o	−0.1	3.0	500.0	70.0	−	3.57	2.68	3.06	2.99	2.95	3.04	−16.7	−9.2	−7.5	−1.7
p	−0.1	3.37	500.0	70.0	−	3.49	2.90	2.92	2.77	3.03	3.23	−20.0	−10.3	−9.7	−3.2
q	−0.043	3.0	500.0	70.0	−	3.47	2.69	2.89	2.86	2.96	3.12	−17.6	−8.6	−8.9	−2.3
r	−0.043	3.37	500.0	70.0	−	3.44	2.72	2.87	2.70	2.92	3.09	−17.6	−8.4	−9.1	−2.5
s†	−0.043	3.37	50.0	10.0	−	8.98	8.98	6.15	9.72	10.08	7.9	134.5	131.5	3.0	−0.2

ε and σ are van der Waals' parameters of the zinc ion. The bond and angle force constants of the zinc ion and its ligands are in kcal/mol·Å^2 and kcal/mol·deg^2, respectively. Possible solvent effects (Solv) near the entrance of the active site are indicated: +, a 14-Å-radius water sphere was added to the mouth of the active site cavity; −, no additional solvent water molecules included. The distances between CO_2 and the nearest atoms of His-119, Val-121, Val-143, Trp-209, the zinc ion, and the zinc-bound OH^- (OH-263) are in Å. The interaction energies of CO_2 with the enzyme and their van der Waals' (vdW), electrostatic (Elec), and metal (Zn) contributions are in kcal/mol.

*Those parameter sets for which the zinc ion leaves its coordination site and CO_2 remains in the hydrophobic binding site.

†Those parameter sets for which CO_2 leaves the hydrophobic binding site.

(parameter sets i and l) and exterior (parameter set s) binding sites. These results suggest that weakening the zinc–ligand interaction would allow wider structural fluctuations around the hydrophobic pocket and eventually lead to CO_2 leaving the hydrophobic binding site. At parameter sets f, g, j, and m (Table 3), both bond and angle force constants between the zinc ion and its ligands are set to zero; the zinc ion is found to leave its coordination site and bind to the side chains of Glu-106, Thr-200, and Tyr-7, whereas CO_2 remains bound in the hydrophobic binding pocket. To prevent leaving of the zinc ion from its coordination site, the σ value of the zinc ion needs to be reduced to $\approx$1.95 Å (parameter set e). These preliminary control calculations indicate that it is crucial to establish a balanced parameter set in the dynamics simulations. For the case of the zinc ion, neglect or assignment of small bond and angle force constants between the zinc ion and its ligands can be compensated by using a smaller σ and/or a more negative ε. Finally, with $\varepsilon = -0.043$ kcal/mol and $\sigma = 3.34$ Å for the zinc ion (parameter sets n and r), inclusion of bulk water molecules at the mouth of the active site has negligible effects on the binding conformation and interactions of CO_2 in the hydrophobic binding pocket.

DISCUSSION

Here we have examined the possible binding sites, binding conformations, and binding interactions of CO_2 in the active site of HCA II. Three potential CO_2 binding sites have been located.§ The first is at the hydrophobic pocket and agrees with expectation based on previous experimental results (see above). The second and the third binding sites occur at $\approx$6 and 10 Å from the zinc ion and may represent intermediate states along the binding pathway of CO_2 into the hydrophobic binding pocket. Our results suggest that along the CO_2 binding pathway, there are at least two energy barriers, which are located near His-64 that connects the inner and outer parts of the active site and at the entrance to the final hydrophobic binding site. In addition, the two CO_2 binding sites outside the hydrophobic pocket may play important roles of CO_2 relay provided, of course, that these two CO_2 binding sites do not interfere with product leaving in the reverse direction. The interaction energies for CO_2 at the exterior and the hydrophobic binding sites are about -17 kcal/mol and are more favorable than that of -9 kcal/mol for the middle CO_2 binding site. Analysis of each possible CO_2 binding site documents that the favorable interaction energy is approximately equally divided between van der Waals' and electrostatic terms at the hydrophobic binding site, while at the middle and the exterior binding sites van der Waals' interaction seems to be more important. In general, the electrostatic interaction increases as CO_2 approaches the positively charged metal ion (Tables 1 and 2).

Although both electrostatic and van der Waals' interactions will direct binding and diffusion of CO_2 in the enzyme's active site, the electrostatic effects of the zinc ion can explain qualitatively some results of our molecular dynamics study. From the radial and angular distribution functions of CO_2 at the three CO_2 binding sites (Fig. 2), we find that fluctuations of Zn—CO_2 distances are $\approx$1 Å and that CO_2 favors a linear binding orientation relative to the zinc ion. To explain the statistically significant preference for a linear binding orientation of CO_2 interacting with the zinc ion, we examined the angular dependence of the electrostatic interaction energies and electrostatic forces between a zinc ion and a CO_2 molecule at fixed Zn—C(CO_2) distances. Fig. 2*C* illustrates the case of Zn—C(CO_2) = 4.0 Å, in which the linear orientation CO_2 ($\tau = 0°$ or 180°) yields the most favorable interaction energy and the largest electrostatic force acting on CO_2 along the Zn–C axis (Fig. 2*C*). These results follow from a classical mechanics and electrostatics treatment of an electronic quadrupole interacting with a point charge. If one assumes polarization of CO_2 to give a nonzero dipole moment for the CO_2 molecule, the analysis is essentially unchanged. Hence, the observed angular distribution of CO_2 in HCA II, which differs significantly from that of a randomly oriented linear molecule (Fig. 2), can be explained in terms of electrostatic interactions between CO_2 and the zinc ion. Of course, interaction of CO_2 with other active site residues may also affect the binding orientation of CO_2.

The significance of the linear binding orientation of CO_2 during CO_2 binding is 2-fold. (*i*) As CO_2 travels from the entrance of the active site cavity to the ultimate binding site at the hydrophobic pocket, a linear CO_2 orientation maximizes the force and, hence, the acceleration of CO_2 toward the zinc ion. (*ii*) In the hydrophobic binding site, the linear binding orientation of CO_2 maximizes the polarization of the CO_2 molecule and, thereby, makes the C of CO_2 more susceptible to nucleophilic attack.¶ Thus, binding of CO_2 in the active site of carbonic anhydrase appears to be a directed process. While interactions of CO_2 with all active site residues are important for stabilizing different intermediate states during the binding process, the zinc ion may be the principal determinant of productive binding and subsequent catalysis.

§It is possible that there could be other CO_2 binding sites along alternate CO_2 diffusion pathways. For example, K. M. Merz (personal communication) has independently identified two CO_2 binding sites that are similar to but not identical with the hydrophobic and middle sites reported herein.

¶In this study, fixed charges were imposed on individual atoms of CO_2, and the polarization effects are, therefore, detected as asymmetry of the C—O bond distances. The C—O bond for the O coordinated to the metal ion is on average $\approx$0.01 Å longer than the other C—O bond. It is expected that the polarization effect on CO_2 due to its binding near the zinc ion would be larger if atomic charges of CO_2 are allowed to vary (7).

We thank Prof. K. M. Merz for early transmission of the results of free energy calculations of CO_2 binding to HCA II. For support of this research we thank the National Science Foundation (CHE-85-15347 and PCM-77-11398) and the National Institutes of Health (GM06920).

1. Eriksson, A. E. (1988) Dissertation (Uppsala Univ., Uppsala, Sweden).
2. Lindskog, S. (1986) in *Zinc Enzymes*, eds. Bertini, I., Luchinat, C., Maret, W. & Zepperzauer, M. (Birkhauser, Boston), pp. 307–315.
3. Lipscomb, W. N. (1983) *Annu. Rev. Biochem.* **52**, 17–34.
4. Pocker, Y. & Sarkanen, S. (1978) *Adv. Enzymol.* **47**, 149–274.
5. Prince, R. H. (1979) *Adv. Inorg. Chem. Radiochem.* **22**, 349–440.
6. Coleman, J. E. (1980) in *Biophysics and Physiology of Carbon Dioxide*, eds. Bauer, C., Gros, G. & Bartels, H. (Springer, Berlin), pp. 133–285.
7. Liang, J.-Y. (1987) Dissertation (Harvard Univ., Cambridge, MA).
8. Liang, J.-Y. & Lipscomb, W. N. (1989) *Int. J. Quantum Chem.* **36**, 299–312.
9. Stein, P. J., Merrill, S. P. & Henkens, R. W. (1977) *J. Am. Chem. Soc.* **99**, 3194–3196.
10. Williams, T. J. & Henkens, R. W. (1985) *Biochemistry* **28**, 2459–2462.
11. Kannan, K. K., Petef, M., Fridborg, K., Cid-Dresdner, H. & Lovgren, S. (1977) *FEBS Lett.* **73**, 115–119.
12. Eriksson, A. E., Kylsten, P. M., Jones, T. A. & Liljas, A. (1988) *Protein* **4**, 283–293.
13. Brunger, A. T., Kuriyan, J. & Karplus, M. (1987) *Science* **235**, 458–460.
14. Elber, R. & Karplus, M. (1987) *Chem. Phys. Lett.* **139**, 375–380.
15. Jorgensen, W. L., Chandrasekhar, J. & Madura, J. D. (1983) *J. Chem. Phys.* **79**, 926–935.
16. Clark, T., Chandrasekhar, J., Spitzagel, G. W. & von Ragué Schleyer, P. (1983) *J. Comp. Chem.* **4**, 294–301.